Implementation of the Cascadia Subduction Zone Source Models for the 2014 Update of the National Seismic Hazard Maps

Rui Chen, Art Frankel, and Mark Petersen
April 2014

In this summary, we describe the implementation of the Cascadia Subduction Zone (CSZ) source models for the 2014 update of the national seismic hazard maps (NSHMs). We also provide tables summarizing key input parameters and a brief explanation of input files for the U. S. Geological Survey (USGS) probabilistic seismic hazard analysis (PSHA) codes. A spreadsheet file containing magnitude-frequency distribution data and rate distribution along CSZ strike can be found in the attachment.

Geometry of the CSZ Ruptures

In the USGS PSHA codes, the 3 dimensional (3D) geometries of potential CSZ interface rupture planes are defined by the surface projections of the potential rupture planes and depth data. The surface projections of rupture planes are delineated by the latitude and longitude coordinates of the surface traces of down-dip and up-dip edges.

The CSZ logic trees have three alternative down-dip edge options (Figures 6 and 7 in Petersen and others, 2014; the latter is reproduced as Figure 1 in this summary for easy references). The geographic extents for these alternative options are shown in Figure 2. The deepest down-dip option, depicted in Figure 2a, represents the top of the non-volcanic tremor zone and is delineated by the average of surface traces compiled by Gomberg and others (2010) and Aaron Wech from http://tunk.ess.washington.edu/map_display/ (Pat McCrory and Luke Blair, written commun., 2012). The middle down-dip option, depicted in Figure 2b, is the average of the 1 cm/yr locking contours from McCaffrey and others (written commun., 2012) and Schmidt and others (written commun., 2012), based on modeling Global Positioning System (GPS) and uplift data and applying a down-dip tapering function derived by Kelin Wang (personal commun., 2012). The shallowest down-dip option, depicted in Figure 2c, is defined by midpoints of fully locked zone from Flück and others (1997), based on thermal modeling and uplift data, and the 1 cm/yr locking contour (i.e., the middle down-dip option depicted in Figure 2b). As discussed in Petersen et al. (2014), the deepest, middle, and shallowest down-dip options are assigned weights of 0.3, 0.5, and 0.2, respectively on the CSZ logic trees for the 2014 NSHMs.

The up-dip edge, depicted in Figure 2d, follows the 5-km depth contour of the 3D digital elevation model (DEM) for the subducting Juan de Fuca Plate beneath western North America developed by Blair and others (2013). Surface traces for the up-dip edge and three down-dip edge options used in the 2014 NSHMs are compared with those used in the 2008 NSHMs in Figure 3, in which dots represent selected points whose latitude and longitude coordinates are used to define the simplified fault traces in the PSHA input files.

Depths at modeled coordinate points shown in Figure 3 were obtained using Arc GIS 3D analysis tools that interpolate depth values for a feature class (modeled points) based on elevation derived from a

terrain dataset, in this case, the subduction interface DEM developed by Blair and others (2013). Coordinates and depth data are given in Table 1.

As discussed in Petersen et al. (2014), a new feature of the 2014 CSZ source model is partial ruptures with smaller magnitudes that supplement the whole CSZ ruptures with moment magnitudes inferred to be about 9.0. These partial ruptures were accounted for using a segmented model and an unsegmented model with equal weights (Figure 1).

The segmented model includes three partial rupture zones in the south and a northern rupture zone. End points for these partial ruptures were chosen as the end points of rupture zones defined by Goldfinger and others (2012) based on their analysis and interpretation of turbidities in deep-ocean cores. The three partial rupture zones in the south correspond to rupture cases B, C, and D in Goldfinger and others (2012, see Figure 4). All three southern rupture zones have the same southern terminus that is also the southernmost end of the CSZ. Latitudes for the northern terminus for partial rupture cases showing in Panels B, C, and D in Figure 4 are 43.7, 45.0, and 46.3 degrees, respectively (Goldfinger, personal commun., 2013). Longitudes for these rupture endpoints were obtained by intersecting the surface traces shown in Figure 3 at the three northern endpoint latitudes (marked on Figure 3). The latitude and longitude coordinates for rupture endpoints are in bold font in Table 1. The northern rupture zone extends from the northern end of Goldfinger's rupture case B to the northern end of the CSZ.

The unsegmented model features a southern CSZ rupture zone and a whole CSZ rupture zone. The unsegmented southern CSZ rupture zone has the same extent as case B in the segmented partial rupture model.

Magnitude Estimations

Potential magnitudes for the full CSZ ruptures (upper logic tree in Figure 1) and for the segmented branch of the partial CSZ rupture logic tree (lower logic tree in Figure 1) were estimated using three global magnitude-area relations developed for subduction zone interface earthquakes: Papazachos and others (2004), Murotani and others (2008), and Strasser and others (2010). These three relations were assigned equal weights. For each of the 4 rupture scenarios shown in Figure 4, we calculated 3D rupture areas in Arc GIS for the three down-dip edge options described in the previous section using up-dip and down-dip surface traces and the subduction interface DEM. Applying the 3 magnitude-area relations to the 3 down-dip edge options resulted in nine different values of magnitude for each rupture scenario for hazard calculations. The 3D rupture areas and calculated magnitudes are given in Table 2. For the full CSZ ruptures (case A in Figure 4), the magnitude ranges from 8.6 to 9.3. The magnitude ranges for the three southern rupture zones (cases B, C, and D in Figure 4) are 8.4 to 9.1, 8.3 to 8.9, and 8.1 to 8.8, respectively. The magnitude range for the northern rupture is 8.3 to 8.9. The magnitude for the unsegmented model on the partial CSZ rupture logic tree varies from 8.0 to 8.7. The 8.0 to 8.7 magnitude range is the same as in the 2008 NSHMs.

Recurrence Rates

For the full CSZ rupture, recurrence rate is the number of events (19) observed by Goldfinger and others (2012) (Figure 4, case A) divided by 10,000 years (the time span of the turbidities in the deep-ocean cores). This ratio yields a rate of 0.0019 per year or a 526-year return period.

For partial ruptures, the logic tree mean rate is 0.0012 per year in the southern CSZ, which is the weighted mean of rates on the three logic tree branches: onshore geologic rate of 0.001 per year; total recurrence rate of 0.0023 per year from Goldfinger and others (2012) for rupture cases B, C, and D; and half of onshore geologic rate (i.e., 0.0005 per year).

For the segmented logic tree branch, rates for rupture cases B, C, and D were determined in a way that maintains the relative rates observed by Goldfinger and others (2012) while honoring the logic tree mean rate (see Table 3). This implementation imposes a partial rupture recurrence rate that varies along the strike in the southern CSZ (Figure 4): 0.0012 per year (total rate of cases B, C, and D) in the southernmost segment (along the length of rupture case D), 0.0006783 per year from northern end of rupture case D to northern end of rupture case C (total rate of cases B, and C), and 0.0002087 from northern end of rupture case C to northern end of rupture case B (rate for case B only). The recurrence rate for the northern rupture zone was chosen to be the same as the onshore geologic rate of 0.001 per year. The logic tree branch with added northern rupture zone has a weight of 0.25. Therefore, the weighted rate is 0.00025 per year in the northern portion of the CSZ (Table 3).

The rate logic tree for southern ruptures in the segmented model is also applied to the southern CSZ logic tree branch in the unsegmented model (Figure 1), i.e., with a mean rate of 0.0012 per year. Rates for the whole CSZ logic tree branch in the unsegmented model is scaled from rates for the southern CSZ by the length ratio of the entire CSZ (1027 km) and the southern zone (665 km). Gutenberg-Richter recurrence law is applied in the unsegmented model, with magnitude ranging from 8.0 to 8.7 in 0.1 increment. In applying Gutenberg-Richter recurrence law, *b* value is fixed at 1 or 0 and the corresponding *a* value is calculated for the given minimum magnitude, maximum magnitude, and event rate. Calculations for the *a* value can be found in the attached spreadsheet.

Magnitude-frequency distribution

Figure 8 in Petersen and others (2014) shows the total accumulative and incremental rates for all ruptures for the entire CSZ. The incremental magnitude frequency distributions are for binned magnitudes with bin width of 0.1 magnitude unit and rates are given at the center of each bin. The CSZ cumulative magnitude frequency distribution implies an effective recurrence time of about 300 years for earthquakes with M $\geqslant$ 8.0. Magnitude-frequency data are available in the attached spreadsheet.

The modeled earthquake rates along the CSZ are dominated by the full characteristic CSZ ruptures, with one event every 526 years. Figure 9 in Petersen and others (2014) shows the contributions to the earthquake rates from each of the models and how the rates vary along the fault. For example, in the far south (adjacent to California) the large earthquake rate is about one event in 315 years, whereas in the

far north (adjacent to Washington) the rate is lower, about one event in 460 years. Data used in plotting earthquake rates along the CSZ are available in the attached spreadsheet.

Notes on Input Files, Weights, and Scaling Factors used in the USGS PSHA FORTRAN Codes

Hazard calculations using the USGS PSHA codes are accomplished in two steps. In the first step, hazards from individual ruptures are calculated separately, one input file for each rupture. In the second step, logic tree weights are applied to the hazards calculated from each input file and the total hazards are obtained by combining (adding) weighted hazards from all input files. Separate input files are also needed when Gutenberg-Richter recurrence law is used with alternative sets of parameters.

There are 27 input files for the CSZ in the PSHA calculations for the 2014 NSHMs. Input filenames for various cases on the CSZ logic trees are appended to the logic tree in Figure 5. In naming the input files, we used terms or abbreviations that are descriptive of the input parameters: “sub0” indicates full CSZ rupture; “sub1”, “sub2”, and “sub3” correspond to rupture extents of cases B, C, and D, respectively; “sub4” is for northern rupture zone in the segmented model; “ch” represents characteristic recurrence law for the segmented model; “grb0” and “grb1” represent Gutenberg-Richter recurrence law with *b* value fixed at 0.0 and 1.0, respectively, for the unsegmented model; and “top”, “mid”, and “bot” are for the shallowest, middle, and deepest down-dip edge options, respectively.

Logic tree branch weights and total weights applied to individual input files are summarized in Table 4. As noted previously, hazards from the full rupture logic tree (top portion in Table 4) and partial CSZ rupture logic tree (middle and bottom portions in Table 4) are additive (each has a total weight of 1.0). Segmented and unsegmented models are two alternative options on the partial CSZ rupture logic tree (each has a total weight of 0.5). In the segmented model, hazards from individual rupture scenarios are additive. The three rupture scenarios (sub1, sub2, and sub3) in the southern CSZ are included in the hazard calculations with full weight; whereas hazards from the northern rupture scenario (sub4) are included with a weight of 0.25. This implementation reflects the two branches on the logic tree node for the inclusion of the northern zone. These two branches are: adding northern zone (weighted 0.25), and no northern zone (weighted 0.75).

The input files for USGS hazard calculations were put together initially for a draft version of the 2014 NSHMs. In that draft version, only the onshore geologic rate (0.001 per year) branch was implemented for the partial CSZ rupture logic tree (i.e., rates in input files are those listed in the 2nd to the last column in Table 3). Rate logic tree branches can be implemented by scaling because ground motion hazard is scaled linearly with recurrence rate. A scaling factor of 1.2 is applied to all input files for ruptures in southern CSZ to achieve the logic tree mean rate of 0.0012 per year. As described previously, for the whole CSZ floating rupture in the unsegmented model, the mean rate observed in the southern CSZ is scaled by the length ratio of full CSZ and southern CSZ, giving an equivalent mean rate of approximately 0.00185 per year (i.e., a scaling factor of approximately 1.85). Hazards for the northern zone (sub4) do not need to be scaled northern zone because its only rate option is 0.001 per year.

In combining the hazards calculated from individual input files using USGS PSHA codes, the final scaling factor for each input file is the total weight for that input file (2nd to the last column in Table 4) times its

rate scaling factor (last column in Table 4). Input files and combine input files are available in the USGS PSHA repository.

References

Blair, J.L., McCrory, P.A., Oppenheimer, D.H., and Waldhauser, F. (2011, revised 2013). A Geo-referenced 3D model of the Juan de Fuca Slab and associated seismicity: U.S. Geological Survey Data Series 633, v.1.2, http://pubs.usgs.gov/ds/633/.

Flück, P., Hyndman. R.D., and Wang, K. (1997). Three-dimensional dislocation model for great earthquakes of the Cascadia subduction zone, J. Geophys. Res., 102, B9, pp. 20,539-20,550, 1997, doi:10.1029/97JB01642.

Goldfinger, C., Nelson, C.H., Morey, A., Johnson, J.E., Gutierrez-Pastor, J., Eriksson, A.T., Karabanov, E., Patton, J., Gracia, E., Enkin, R., Dallimore, A., Dunhill, G., and Vallier, T. (2012). Turbidite Event History: Methods and Implications for Holocene Paleoseismicity of the Cascadia Subduction Zone, USGS Professional Paper 1661-F, Reston, VA, U.S. Geological Survey, 332 p, 64 Figures.

Goldfinger C. (2013). Personal communication.

Gomberg, J., Bedrosian, B., Bodin, P., Bostock, M., Brudzinski, M., Creager, K., Dragert, H., Egbert, G., Ghosh, A., Henton, J., Houston, H., Kao, H., McCrory, P., Melbourne, T., Peacock, S., Roeloffs, E., Rubinstein, J., Schmidt, D., Trehu. A., Vidale, J., Wang, K., and Wech, A. (2010). Slow-slip phenomena in Cascadia from 2007 and beyond; a review, Geol. Soc. Am. Bull., v. 122, pp. 963-978.

McCaffrey P. (2012). Personal communication.

McCrory P., and Blair L. (2012). Written communication.

Murotani, S., Miyake, H., and Koketsu, K. (2008). Scaling of characterized slip models for plate-boundary earthquakes: Earth, Planets, and Space, v. 60, p. 987-981.

Papazachos, B.C., Scordilis, E.M., Panagiotopoulus, C.B., and Karakaisis, G.F. (2004). Global relations between seismic fault parameters and moment magnitudes of earthquakes, Bulletin of the Geological Society of Greece, v. 36. , pp. 1482-1489.

Petersen, M.D., Moschetti, M.P., Powers, P., Mueller, C.S., Haller, K.M., Frankel, A.D., Zeng, Y., Rezaeian, S., Harmsen, S.C., Boyd, O.L., Field, N., Chen, R., Rukstales, K.S., Luco, N., Wheeler, R.L., and Olsen, A.H. (2014). Documentation for the 2014 National Seismic Hazard Maps: U.S. Geological Survey Open-File Report, in review

Schmidt and others. (2012). Written communication.

Strasser. E.O., Arango, M.C., and Bommer, J.J. (2010). Scaling of the source dimensions of interface and intraslab subduction-zone earthquakes with moment magnitude, Seism. Res. Letts, v.81, pp. 951-950.

Wang, K. (2012). Personal communication.

Table 1. Geographic Coordinates and Depths for CSZ Ruptures

Down-dip edge									Up-dip edge		
Top of non-volcanic tremor zone (deepest option)			1 cm/yr locking contour (middle option)			Midpoint of fully locked zone and 1 cm/yr locking contour (shallowest option)					
longitude	latitude	depth (km)	longitude	latitude	depth (km)	longitude	latitude	depth (km)	longitude	latitude	depth (km)
-126.688	49.798	-26.481	-126.828	49.737	-23.691	-127.043	49.619	-19.120	-127.645	49.253	5
-125.859	49.387	-30.035	-126.175	49.214	-22.975	-126.383	49.096	-18.475	-127.080	48.689	5
-125.112	49.039	-32.420	-125.439	48.861	-25.034	-125.749	48.717	-19.011	-126.678	48.278	5
-124.458	48.658	-32.735	-124.804	48.553	-27.841	-125.214	48.413	-21.240	-126.439	47.992	5
-123.917	48.255	-32.443	-124.361	48.152	-27.869	-124.741	48.052	-22.808	-126.234	47.663	5
-123.509	47.780	-33.814	-123.916	47.709	-29.320	-124.334	47.627	-24.469	-126.049	47.279	5
-123.357	47.313	-34.714	-123.899	47.238	-27.913	-124.289	47.183	-23.127	-125.920	46.943	5
-123.352	46.835	-34.745	-124.116	46.779	-23.949	-124.405	46.758	-20.000	-125.816	46.629	5
-123.399	46.377	-34.884	-124.138	46.364	-22.909	-124.432	46.359	-18.595	-125.736	46.330	5
-123.413	**46.300**	**-34.828**	**-124.137**	**46.300**	**-22.928**	**-124.439**	**46.300**	**-18.441**	**-125.729**	**46.300**	**5**
-123.599	45.501	-33.129	-124.330	45.489	-20.210	-124.549	45.485	-16.708	-125.574	45.452	5
-123.702	**45.000**	**-30.998**	**-124.488**	**45.000**	**-17.459**	**-124.561**	**45.000**	**-16.309**	**-125.527**	**45.000**	**5**
-123.734	44.757	-30.306	-124.356	44.742	-19.362	-124.567	44.738	-15.667	-125.500	44.712	5
-123.764	43.882	-29.481	-124.492	43.863	-15.988	-124.630	43.858	-13.991	-125.427	43.841	5
-123.780	**43.700**	**-28.552**	**-124.509**	**43.700**	**-15.277**	**-124.631**	**43.700**	**-13.573**	**-125.411**	**43.700**	**5**
-123.809	42.996	-26.805	-124.514	42.980	-13.663	-124.638	42.975	-11.959	-125.289	42.957	5
-123.662	42.119	-27.892	-124.390	42.112	-12.127	-124.543	42.108	-9.928	-125.047	42.099	5
-123.329	41.215	-29.255	-124.173	41.218	-14.836	-124.348	41.214	-12.702	-125.085	41.214	5
-122.945	40.376	-37.830	-123.829	40.347	-24.018	-124.042	40.347	-22.818	-125.099	40.355	6.745

Note: Entries in bold fonts are northern end points of ruptures.

Table 2. Rupture Areas and Magnitudes

Rupture Scenario	Down-dip Option	3D Rupture Area (km^2)	Papazachos et al. (2004)	Strasser et al. (2010)	Murotani et al. (2008)
Case A	Shallowest	84607.28	9.01	8.61	8.72
	Middle	106110.90	9.12	8.69	8.82
	Deepest	163956.66	9.34	8.85	9.01
Case B	Shallowest	44503.94	8.68	8.37	8.44
	Middle	53789.88	8.78	8.44	8.53
	Deepest	94868.05	9.07	8.65	8.77
Case C	Shallowest	31917.12	8.52	8.25	8.30
	Middle	39003.30	8.62	8.33	8.39
	Deepest	71176.63	8.92	8.55	8.65
Case D	Shallowest	21797.47	8.32	8.11	8.13
	Middle	26703.54	8.43	8.19	8.22
	Deepest	51055.54	8.75	8.42	8.50
Northern	Shallowest	40103.34	8.63	8.34	8.40
	Middle	52321.02	8.77	8.43	8.52
	Deepest	69088.62	8.91	8.54	8.64

Magnitude-Area Relations:

Papazachos et al. (2004): $\log S = 0.86M - 2.82$

Strasser et al. (2010): $M = 4.441 + 0.846 \log S$

Murotani et al. (2008): $S = (1.48 \times 10^{-10})(M_o)^{\frac{2}{3}}$, where M_o is moment in Nm (to convert to magnitude use log M_o= 1.5M + 9.05)

Table 3. Recurrence Rate Calculations

Rupture Cases			M range	Rate based on Goldfinger and others (2012)			Onshore geologic rate of 0.001 per yr[4]	Logic tree mean rate (per yr)[5]
				Number of Events in 10,000 yrs[1]	Rate (per yr)	Recurrence (yr)		
characteristic (segmented)	full CSZ (case A)		8.6 – 9.3	19	0.00190	526	-	0.0019
	partial rupture	case B	8.4 – 9.1	4	0.00040	2500	0.0001739[1]	0.0002087
		case C	8.3 – 8.9	9	0.00090	1111	0.0003913[1]	0.0004696
		case D	8.1 – 8.8	10	0.00100	1000	0.0004348[1]	0.0005217
		total of B, C, D	-	23	0.0023		0.001	0.0012
		northern zone	8.3 – 8.9	-	-	-	0.001	0.00025[2]
Gutenberg-Richter (unsegmented)		full CSZ	8.0 – 8.7	-	-	-	0.001	0.0019[3]
		southern CSZ	8.0 – 8.7	-	-	-	0.001	0.0012

[1]Calculated using the rate of Goldfinger and others (2012) (in third column) times the ratio of onshore geologic rate (0.001) and the total rate (0.0023) of cases B, C, and D by Goldfinger and others (2012).

[2]Onshore geologic rate of 0.001 per year times the logic tree branch weight of 0.25.

[3]Southern rupture rate of 0.0012 times 1.5445 (ratio of the total CSZ length of 1027 km and the southern CSZ length of 665 km).

[4]Used directly in the input files to calculate draft 2014 NSHMs.

[5]Used in the final NSHMs, these logic tree mean rates were achieved by scaling hazards calculated from input files.

Table 4. CSZ Logic Tree Weights and Rate Scaling Factors for Hazard Calculations

Full CSZ rupture (Characteristic, Case A)	**Down-dip edge options**	**Total weight**	**Rate Scaling**
sub0_ch_bot	0.3	0.3	none
sub0_ch_mid	0.5	0.5	
sub0_ch_top	0.2	0.2	

Unsegmented model (Partial rupture)	**Unsegmented**	**Whole or southern**	**b-value (1 or 0)**	**Down-dip edge**	**Total weight**	**Rate scaling**
sub0_GRb0_bot	0.5	0.25	0.5	0.3	0.01875	1.8534
sub0_GRb0_mid				0.5	0.03125	1.8534
sub0_GRb0_top				0.2	0.01250	1.8534
sub0_GRb1_bot			0.5	0.3	0.01875	1.8534
sub0_GRb1_mid				0.5	0.03125	1.8534
sub0_GRb1_top				0.2	0.01250	1.8534
sub1_GRb0_bot		0.75	0.5	0.3	0.05625	1.2
sub1_GRb0_mid				0.5	0.09375	1.2
sub1_GRb0_top				0.2	0.03750	1.2
sub1_GRb1_bot			0.5	0.3	0.05625	1.2
sub1_GRb1_mid				0.5	0.09375	1.2
sub1_GRb1_top				0.2	0.03750	1.2

Segmented model (Partial rupture)	**Segmented**	**Inclusion**	**Down-dip edge**	**Total weight**	**Rate scaling**
sub1_ch_bot.pga.out	0.5	1.0	0.3	0.15	1.2
sub1_ch_mid.pga.out			0.5	0.25	1.2
sub1_ch_top.pga.out			0.2	0.10	1.2
sub2_ch_bot.pga.out	0.5		0.3	0.15	1.2
sub2_ch_mid.pga.out			0.5	0.25	1.2
sub2_ch_top.pga.out			0.2	0.10	1.2
sub3_ch_bot.pga.out	0.5		0.3	0.15	1.2
sub3_ch_mid.pga.out			0.5	0.25	1.2
sub3_ch_top.pga.out			0.2	0.10	1.2
sub4_ch_bot.pga.out	0.5	0.25	0.3	0.0375	none
sub4_ch_mid.pga.out			0.5	0.0625	
sub4_ch_top.pga.out			0.2	0.0250	

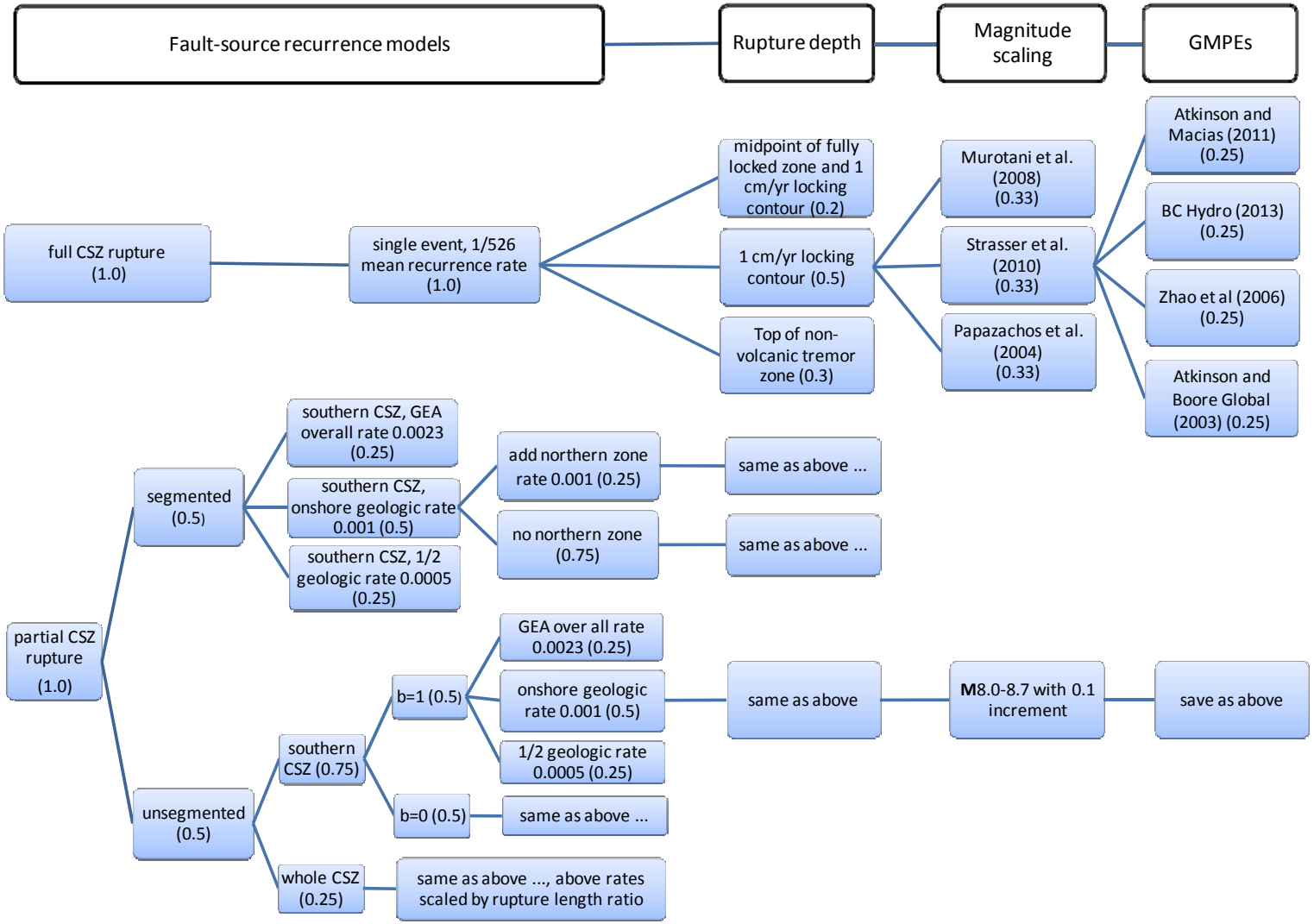

Figure 1. CSZ summary logic tree (after Petersen and others, 2014). Note that the hazard (frequency of exceeding any given ground motion) from full CSZ ruptures and partial ruptures is additive. Weight for each branch is given in parentheses. The magnitude scaling branches apply to all three rupture depth branches. Ground motion attenuation prediction equation (GMPE) branches apply to all magnitude scaling branches as well as all branches in the unsegmented model. Text “same as above” with ellipsis implies that the box directly above as well as all boxes thereafter apply to the current branch. GEA denotes the Goldfinger and others (2012) rupture rate.

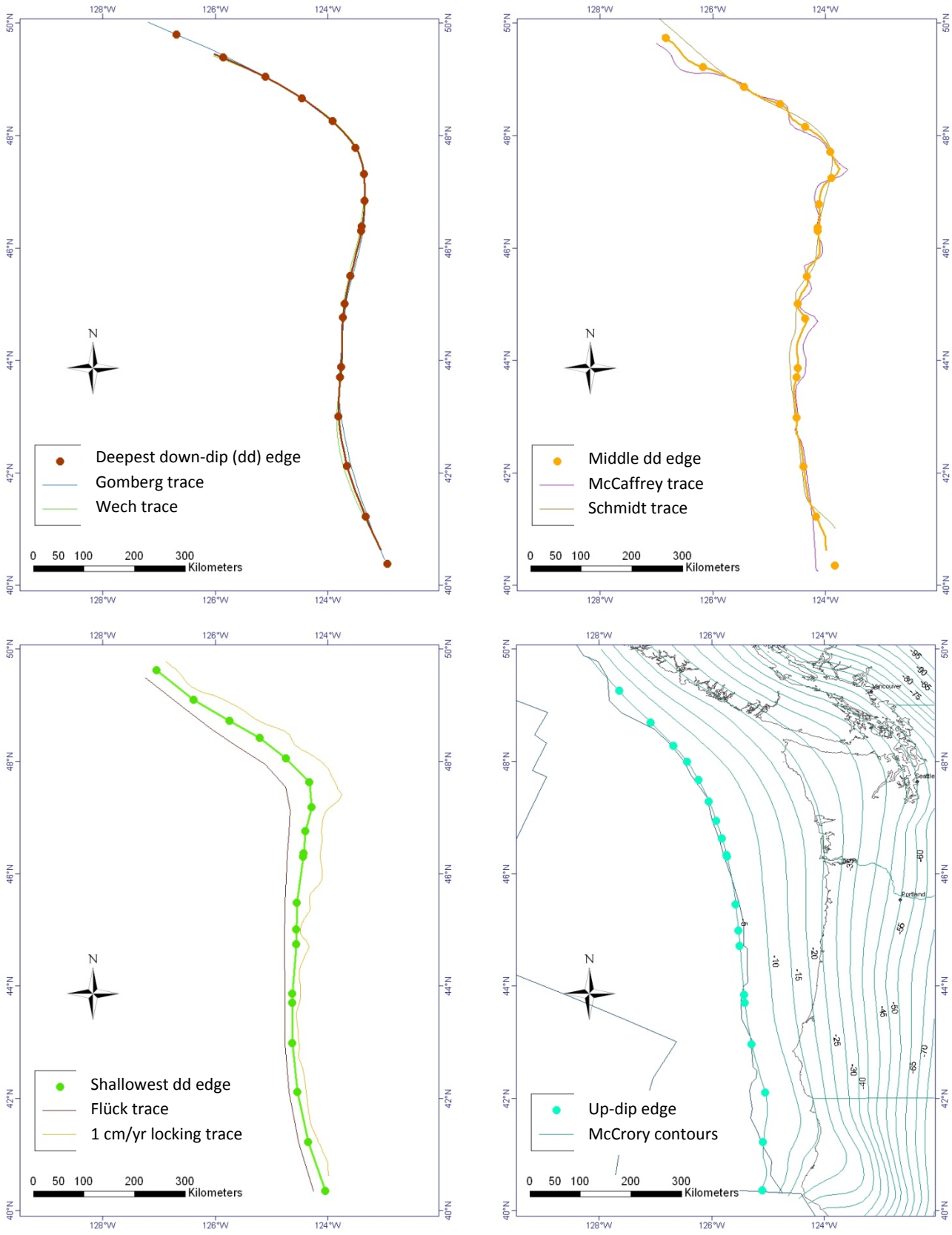

Figure 2. Surface traces of the three down-dip edge options and the up-dip edge for the CSZ. Dots represent selected points 3 dimensional coordinates (latitude, longitude and depth) are used to define the simplified rupture planes in PSHA calculations.

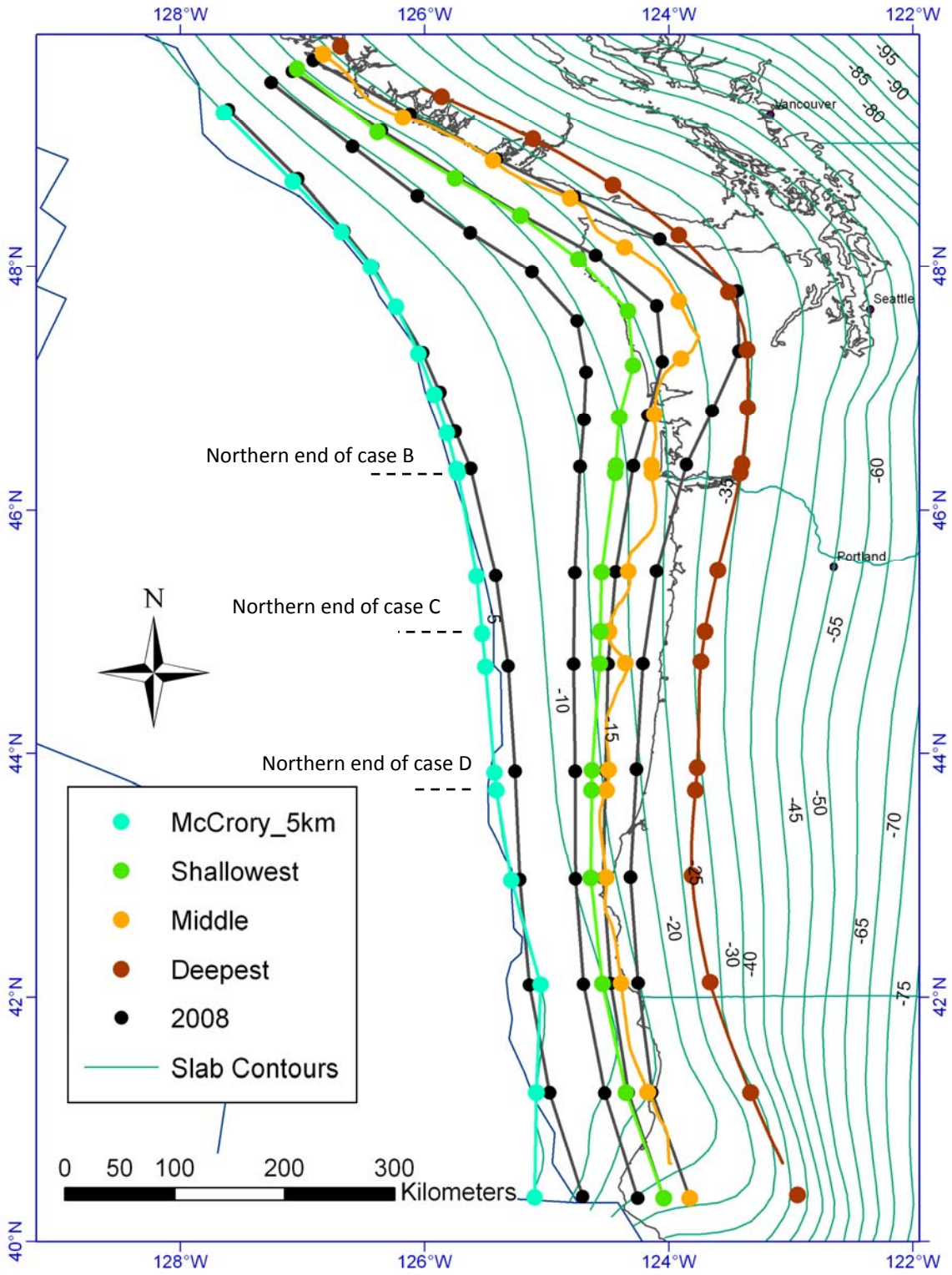

Figure 3. Comparison of surface traces for the up-dip edge and three down-dip edge options used in the 2014 NSHMs with those used in the 2008 NSHMs. Dots represent selected points whose 3D coordinates (latitude, longitude, and depth) are used to define the simplified fault traces in the PSHA input files. These coordinates are given in Table 1.

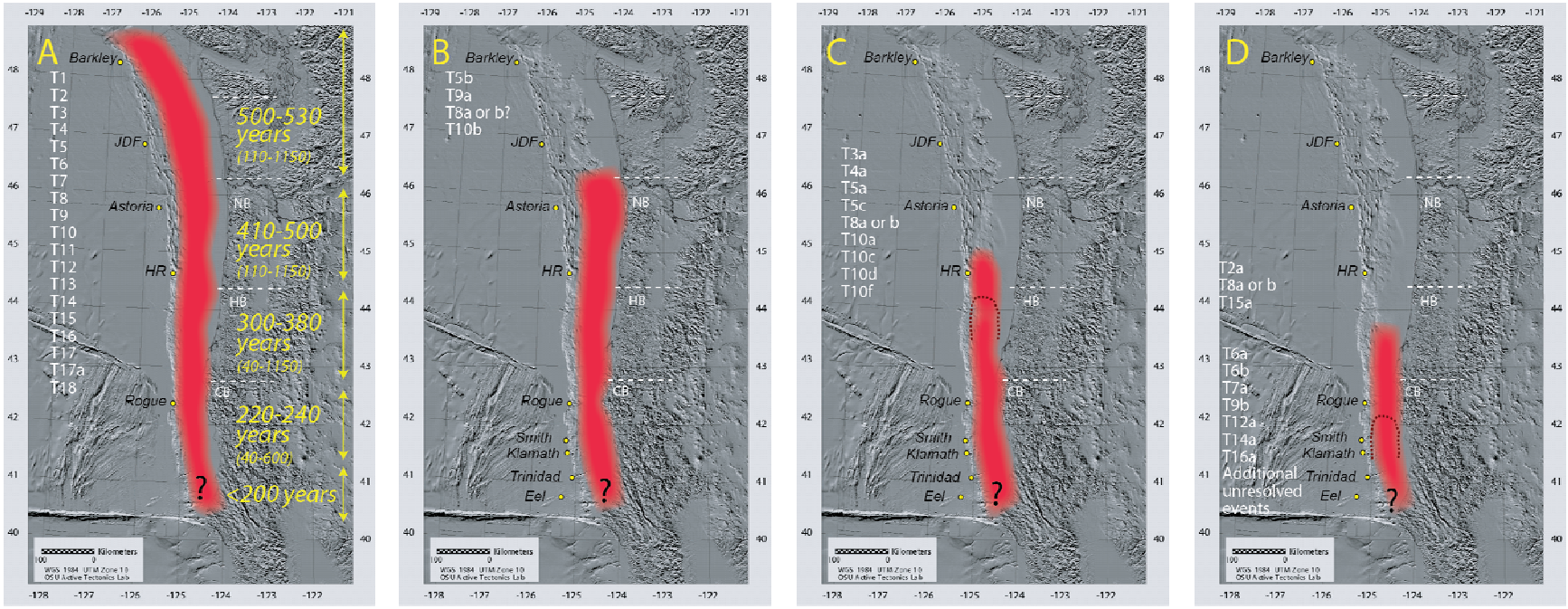

M8.6 - 9.3
526 yrs

M8.4 - 9.1
2,500 yrs

M8.3 - 8.9
1,111 yrs

M8.1 - 8.8
1,000 yrs

Figure 4. Figure taken from Goldfinger and others (2012) showing rupture zones of great Cascadia earthquakes that they determined from the turbidite record over the past 10,000 yr. Black dots are locations of cores. Designation of great earthquakes for each rupture scenario is given on left side of each panel (*e.g.*, T1, T5b). CB = Cape Blanco. HB = Heceta Bank. NB = Nehalem Bank. We have added at the bottom the preferred magnitude range and recurrence time used for each rupture scenario in our implementation of the Goldfinger and others (2012) rupture model. Recurrence times are determined by dividing 10,000 yr by the number of earthquakes in that scenario.

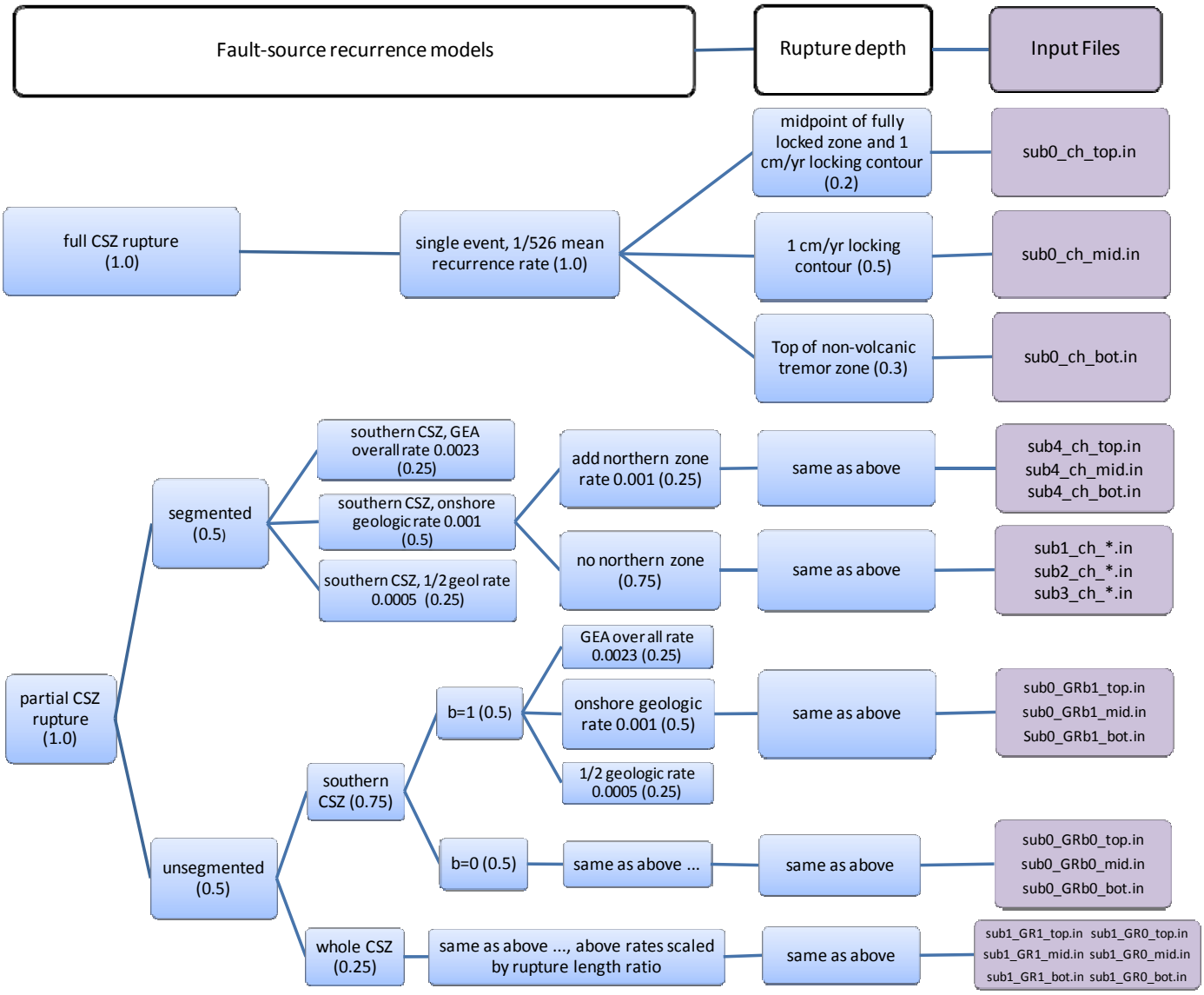

Figure 5. CSZ logic trees with input filenames for probabilistic ground motion hazard calculation using USGS FORTRAN codes.